AIAA IAC-02-I.1.07

Experimental Testing of Tape Springs Folded in Three Dimensions

Scott J.I. Walker and Guglielmo Aglietti
School of Engineering Sciences, University of Southampton, UK

53rd International Astronautical Congress
The World Space Congress - 2002
10-19 Oct 2002/Houston, Texas

Experimental Testing of Tape Springs Folded in Three Dimensions

Scott J.I. Walker* and Guglielmo Aglietti†
School of Engineering Sciences, University of Southampton, UK

One of the main drivers in satellite design is the minimization of mass, in the attempt to reduce the large costs involved in the launch of the spacecraft, and the recent advances in micro electro mechanical systems (MEMS) have allowed a further reduction in the mass of on-board equipment. With advances in micro ion propulsion systems for attitude control, and the miniaturization of ground based mobile communications, the satellite power requirement does not reduce linearly with mass. This creates the need for photovoltaic cell areas larger than the external surface area of the satellite bus. Therefore small satellite deployable structures become increasingly important. The major design requirements for such systems are reliability and low cost. The simpler the components of the system are (i.e. the minimum number of moving parts, lubrication etc), the more chance of the system meeting the design requirements. For this reason, there has been significant investigation into the deployment dynamics of tape springs folded in two dimensions, to form simple hinges which do not require lubrication and automatically lock in the deployed configuration. The present work focuses on using tapes springs to support a new conceptual area deployment design for nano/micro satellites. The deployment of this design incorporates bi-axial folding, which requires the tape springs to unfold in three dimensions. Little research has been carried out in this area. The design of a test rig to determine the properties of this three dimensional deployment is presented in detail. This rig measures both the bending and twisting moments produced from the three-dimensional fold. The combination of these two moments defines the main deployment properties of the tape springs and hence the final array. The experimental results will be compared to theoretical results produced using shell theory and non-linear, finite element analysis.

Nomenclature

D	Flexural Rigidity
ν	Poisson's Ratio
α	Angle subtended by cross-section of spring
t	Thickness of the tape spring
θ	Total fold angle
M	Bending moment applied to the strip (about y axis)
M_+^{max}	Peak moment for opposite sense bending
M_-^{max}	Peak moment for equal sense bending
M_+^*	Steady state moment for opposite sense bending
M_-^*	Steady state moment for equal sense bending
T^{max}	Maximum torsional moment
R_L	Initial longitudinal radius of curvature
R_T	Initial transverse radius of curvature
κ_x	Change in longitudinal curvature
κ_{xy}	Change in twisting curvature

Introduction

OVER the last fifteen years there has been growing research and advances in the miniaturization of electronic and mechanical technologies (for example, micro sun sensors, micro-gyroscopes etc[1]). It is now possible to construct satellites weighing only a few kilograms, thereby dramatically reducing the cost of access to space. Such development opens up many new possibilities for space exploration at low cost for a far wider community of scientists and businesses. In-fact, many nations have identified nano-technology as a critical technology underpinning advances across many market sectors. However, as the total satellite mass reduces, the power requirement of the satellite, in many applications, does not reduce at the same rate. For example, the small size of cellular telephones and hand held receivers for the Global Positioning Satellite (GPS) navigation system creates a need for larger antenna sizes in the space-based components of the system. Greater capacity requires greater on-board power, provided by deployed solar arrays. There is also ongoing research into the use of ion propulsion systems, as primary and secondary propulsion for small satellites, due to their low mass potential. Such systems would also significantly increase the power requirement of the satellite. Usually micro and nano satellites employ body mounted solar cells, however, there is growing interest in deploying photovoltaic cell areas larger than the surface area of the bus face.[2] In such applications the photovoltaic cells would be mounted on a blanket (as opposed to composite pan-

*Graduate Student, Astronautics Research Group
†Lecturer in Aerospace Structural Dynamics, Astronautics Research Group

els) due to the extreme low mass requirement. The critical component of these systems would therefore be the supporting structure of the array. The structure needs to be strong enough to withstand the launch loads, meet the deployed stiffness requirements of the array, have very low mass and deploy with high reliability. Two concepts currently exist that offer a structural solution in this application: inflatable structures and tape springs.

This study focuses on the experimental analysis of tape springs which are folded in three dimensions. Such folds would generally exist in arrays incorporating biaxial folding in their deployment.[2]

The Physics of Tape Spring Bends

Tape springs are defined as thin metallic strips with a curved cross section, which have the key property that they are continuous (i.e. contain no mechanical hinges or other folding devices) and yet they can still be folded elastically. In standard two dimensional tape spring analysis, the springs are loaded by a pair of equal and opposite bending moments, M, which cause them to bend in the 'soft' plane of bending as shown in figure 1 (where R_L, R_T are the longitudinal and transverse radii of curvature of the tape spring). The general sign convention is that a positive bending moment induces tensile stresses along the edges.[3] The

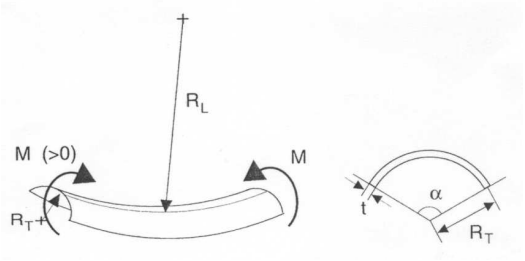

Fig. 1 Tape spring subject to M>0, and its cross-section[3]

bending induced by this positive moment is known as opposite-sense bending because it produces a change of longitudinal curvature that is of opposite sense to the initial transverse curvature of the of the tape spring. Conversely, a negative bending moment induces compressive stresses along the edges of the spring, and is referred to as equal-sense bending. The corresponding longitudinal rotation of the tape spring, θ, (which is positive, for a positive applied moment) is the key deformation parameter in this study.

For two dimensional analysis the general moment-rotation relationship is shown in figure 2 (where M_+^{max}, M_-^{max} are the peak moments for opposite-sense and equal-sense bending and M_+^*, M_-^* are the steady-state moments for opposite-sense and equal-sense bending.) It can be seen that the tape spring snaps through at A and B.

A three dimensional tape spring bend has both bending and twisting properties (see figure 3). If one end

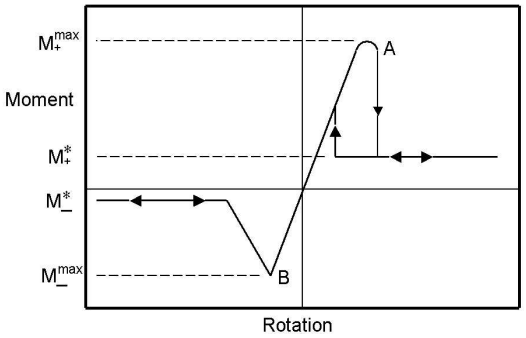

Fig. 2 Graph of Moment-Rotation relationship for a straight tape spring

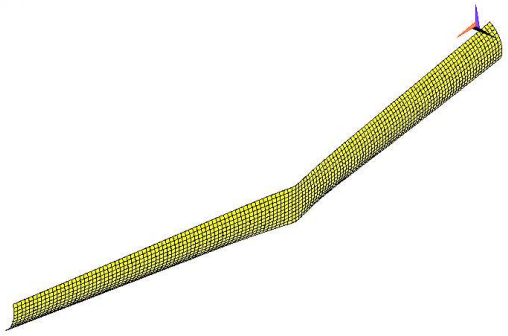

Fig. 3 3D Bend (10° bend, 20° twist per end)

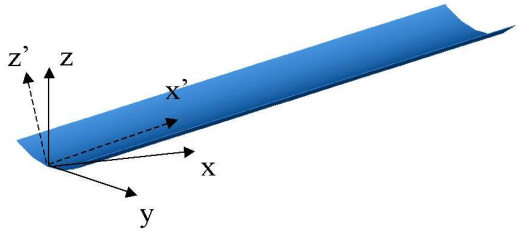

Fig. 4 Moving Co-ordinate System

of a tape spring is completely fixed in space then any movement of the other end, to any location (bent about a central fold) can be reproduced experimentally by applying a rotational displacement about the y axis (bending) and a rotational displacement (twisting) about, what is initially the x axis (see figure 4). For these experimental tests it should be noted that when a rotational displacement is applied about the y axis, the x axis remains in the plane of the initial undisplaced tape spring. The axes x' and z' however rotate around the y axis so that the x' axis remains in the plane of the displaced tape spring (see figure 4). Therefore, twisting occurs around the x' axis. It has been observed that twisting the tape spring greatly impacts the buckling load of both equal and opposite sense bends. From previous work[4] it is known that equal sense bends fail via a torsional buckling mode, whereas opposite sense bends fail through a bending 'snap through' mode. Therefore it is known that twisting reduces the buckling load of an equal sense bend, and increases the buckling load of an opposite sense

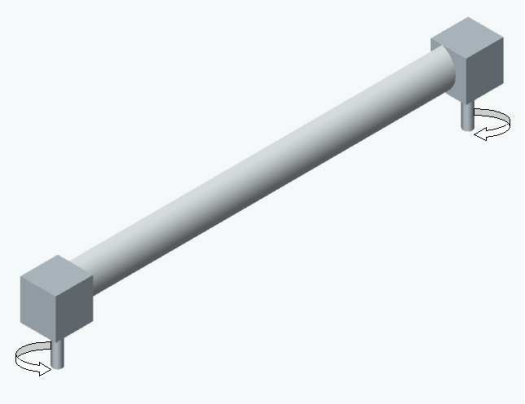

Fig. 5 Basic Layout of 2D Bend Test Rig

bend.

Test Rig Design

The aim of the experimental campaign was to measure the bending and twisting moments created when a tape spring is folded in three dimensions. Such three dimensional bends require dual axis rotation about each tape spring end. Two factors initially determine the basic design of the test rig. The first is that due to the non-linear nature of the folds, rotational displacements (not forces) need to control the motion of the system. Secondly, from figure 3, it can be seen that one end of the tape spring should have two free degrees of freedom (rotation about the y and x' axes) and the other end needs three degrees of freedom (rotation about the y and x' axes and displacement along the x axis). This suggests a moving end and a fixed end of the rig (as can be seen in the 2D test rig in Fischer[5] (1995)). Rotational displacements would then be applied around y and x', and the displacement along x would occur in response to the rotational inputs. Current 2D test rigs, simply enable rotation about the y axis and linear movement along x, as can be seen in figure 5. The longitudinal moments created by the two dimensional fold are measured using strain gauges mounted on the y axle. For the three dimensional test rig, the supporting structure became more complex due to the added rotational degree of freedom required for each end of the tape spring. The initial design aim was to ensure that the rotational displacements applied to the ends of the tape spring, did not result in any translational displacements of the tape spring ends, see figure 6. From this diagram, it is clear that the twist axle (x' axis) needed to be mounted on a secondary support structure which rotated about the y axle. This rotating structure can be seen in figure 7. This structure was designed so that the weight created at the twist axle mounting could be balanced by weights mounted on the front of the structure. This ensures that moments measured in the y axle were created only by the tape spring fold. In practice this structure was not perfectly balanced, therefore the additional moment produced by the unbalance was measured in a pre-test and subtracted from the test results. This procedure was also performed for the twist axis to ensure the results were as accurate as possible. Each of the two rotating structures were mounted on vertical supports allowing the y rotation. One set of vertical supports were attached to a base board, forming the fixed end of the test rig. The other set of vertical supports were mounted on a rolling carriage which was free to run along a track, mounted on the base board. The linear movement of the carriage was laterally restricted by the use of a 'v' track, to ensure all movement occurred solely in the x direction. All the bearings used in the moving carriage (and each rotational degree of freedom) were low friction bearings with the minimum static friction torque. The vertical supports, carriage and base board can be seen in figure 8. The base board was sized to test tape spring lengths of up to 50cm. The total supporting structure is shown in figure 9. The most critical area of the design was the measurement system. The sensors detecting the reaction moments about y had to measure, with accuracy (within 5% of the mean result), values ranging from 20 to 1000+ Nmm. Whereas the sensors detecting the reaction moments about x' had to measure, with accuracy (again, within 5% of the mean result), values ranging from around 1 to 25Nmm. The commercially available solution to measure moments about an axis are torque transducers. However these were an unfeasible solution to the problem due to the dimensions available and the expected torque range. The chosen solution was to transmit the ro-

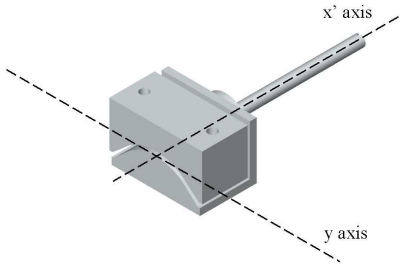

Fig. 6 Required Rotation

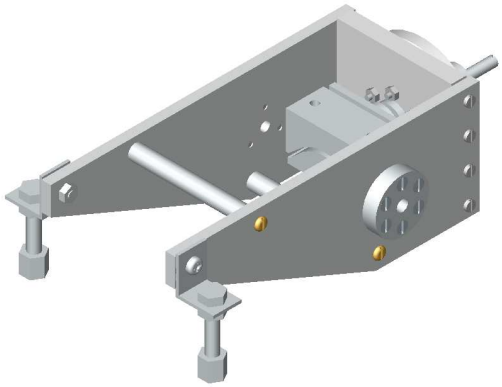

Fig. 7 Rotating Structure

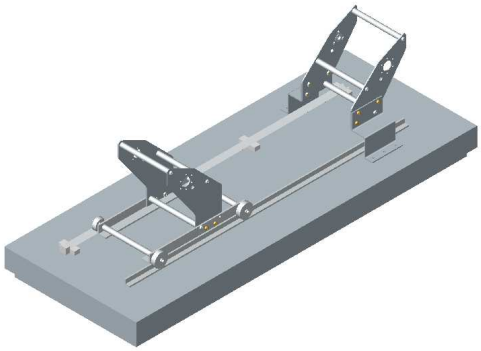

Fig. 8 Base Structure

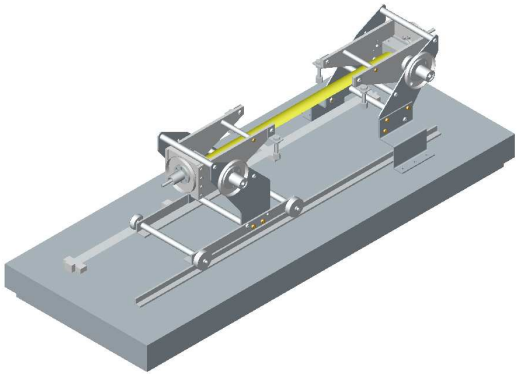

Fig. 9 Total Structure

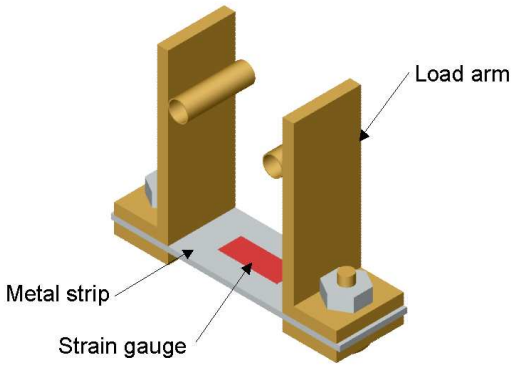

Fig. 10 Strain Gauge Unit (SGU)

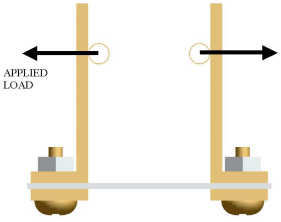

Fig. 11 Loaded Strain Gauge Unit

tational loads through a strain gauge unit (SGU), (a computer generated model of which can be seen in figure 10). The unit consists of two load arms bolted to a metal strip. As a load is applied to the load arms (see figure 11), the strip bends, producing a strain. The magnitude of this strain is measured by a strain

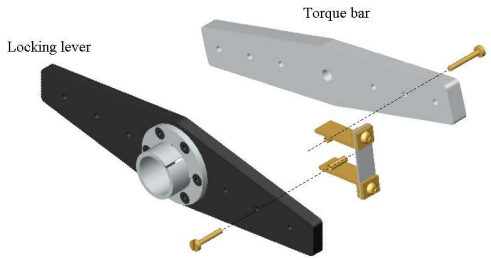

Fig. 12 Exploded view of measurement system layout

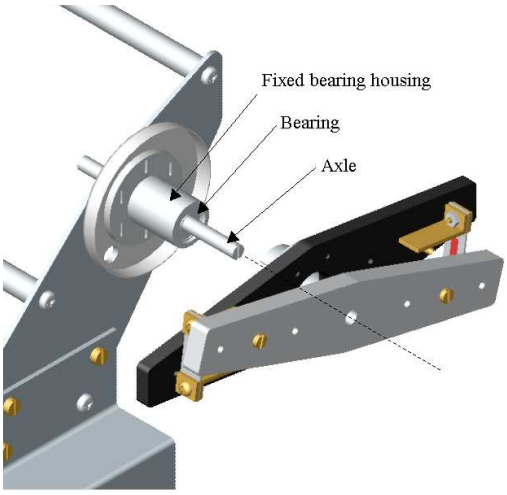

Fig. 13 Exploded view of the y axle layout

gauge mounted on the surface of the strip. This unit connects to a 'locking lever' (mounted independently from the rotating axle, to lock the displacement) and a 'torque bar' (fixed to the rotating shaft), see figure 12. Therefore, any moment from the tape spring is transmitted as a force across the arms of the strain gauge unit. The magnitude of the measured strain can be varied by one, or a combination of three ways.

- By altering the dimensions of the test strip (thickness, width)
- By altering the radial mounting location of the strain gauge unit
- By altering the number of strain gauge units mounted around an axle

A locking lever and torque bar is mounted on each axis of rotation as shown in figure 13. The locking lever is mounted on a fixed bearing housing which, contains two bearings at the ends of the housing to support the axle. The torque bar is locked on to the axle. To ensure experimental accuracy, the SGU's were individually loaded and unloaded with known forces, resulting in a load-voltage relationship (equivalent to a load-strain relationship) with an accuracy within 5% of the mean result.

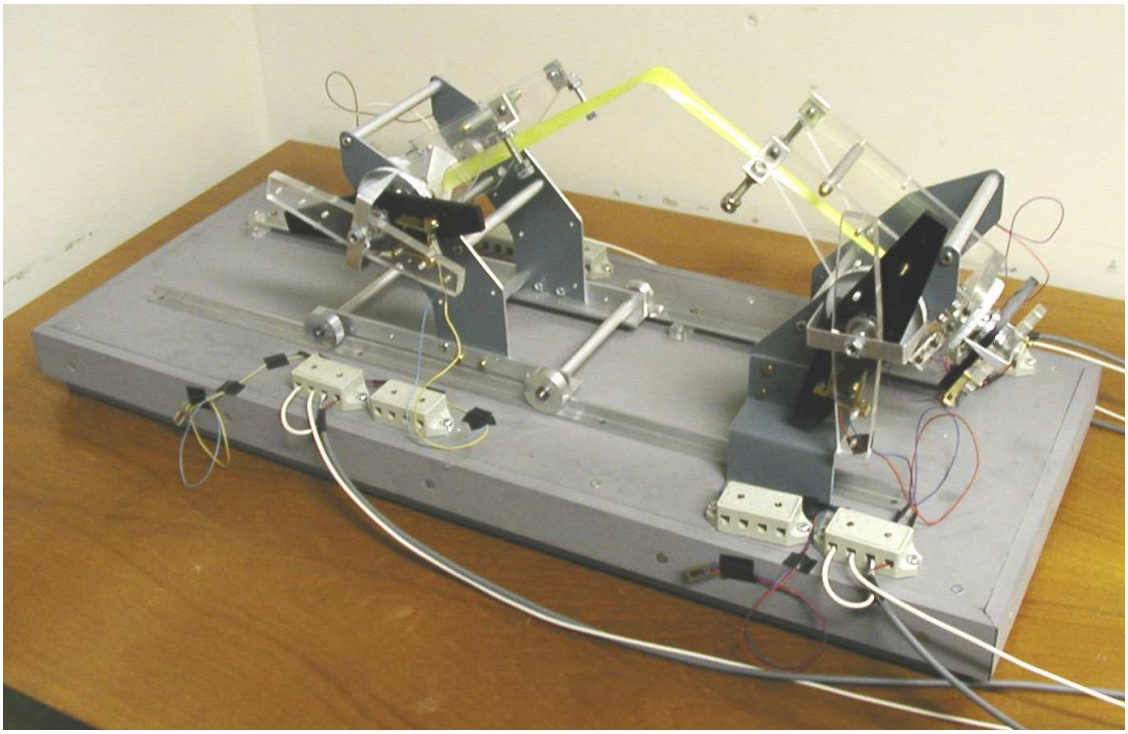

Fig. 14 Photograph of Test Rig

Steps were taken to minimize sources of error, not only in the mechanical system but also in the electrical system. To avoid temperature drift from the strain gauges, temperature compensating (half bridge) circuits were used.
The eight circuits were connected to eight channel inputs of a strain gauge amplifier which were, in turn, connected to a computer. The data was captured statically, and for every capture, 100 samples from each channel was taken.
A photograph of the test rig in use can be seen in figure 14.

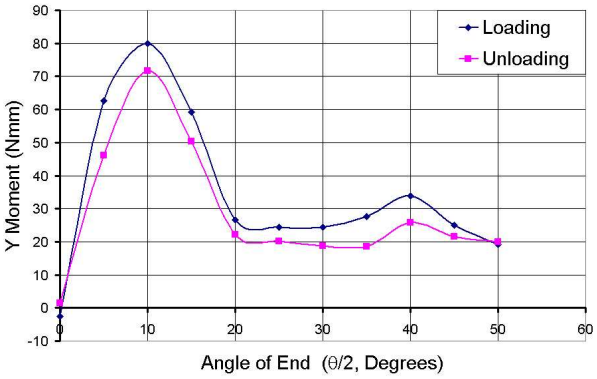

Fig. 15 Equal Sense 2D Bend

Initial Results

The initials tests were performed on a 400mm long tape spring made from 0.11mm thick, AISI 1095 steel. The tape spring had an initial transverse radius of curvature (R_T) of 20mm and an initial cross sectional angle of embrace (α) of 1.25 rad. Two dimensional bends were used to investigate the accuracy of the experimental results produced from the test rig. Testing was initially performed using two Y SGU's on each axle. With two voltage results per axle, a comparison between the two could increase the accuracy of the measured moment. However it was found that the moments created by the fold under the loading conditions were predominantly very small. As the inaccuracy of the SGU's increased as the measured strain reduced, it was decided that more accurate results could be obtained using only one Y SGU per axle (doubling the load across the test strip).
Figure 15 shows the loading and unloading moment-rotation relationship for a two dimensional equal sense bend. These results predict a peak equal sense moment (M_{-}^{max}) of 80Nmm and an average steady state moment (M_{-}^{*}) of 23.25Nmm. (M_{-}^{max} is found from the loading relationship as it is known that the unloading relationship results in a lower peak.[3])
Figure 16 displays the unloading moment-rotation relationship for a two dimensional opposite sense bend. It was found that due to the experimental test increment angle of 5° per end, the peak opposite sense moment could not be determined accurately. Therefore, these initial experimental tests focused on unloading opposite sense bends. From figure 16, it can be seen that no unloading peak moment occurs. This is because the snap back occurs when $\theta < 10°$. This result predicts an average opposite sense steady state moment (M_{+}^{*}) of 41.75Nmm.
Three dimensional testing was unexpectedly restricted

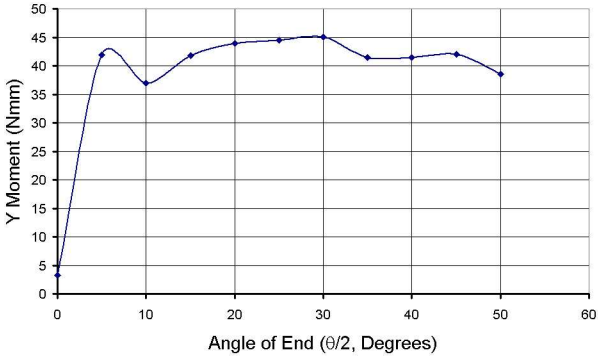

Fig. 16 Opposite Sense 2D Bend

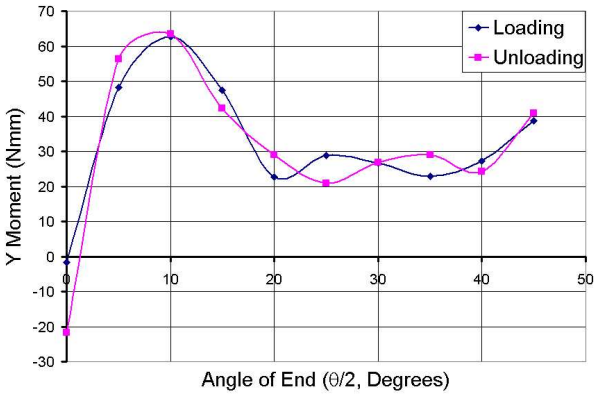

Fig. 17 Equal Sense 3D Longitudinal Moment

by the limitation that only one SGU could be used on each twist axle. Due to the higher loads, it was calculated that opposite sense three dimensional bends would strain the bending metal strips (in the SGU's) past their yield point. Therefore, tests were limited to equal sense three dimensional bends. All tests were performed with an ideal bend twist relationship. I.e. the end twist angle throughout the tests would remain twice as large as the end bend angle. This results in a final longitudinal bend (θ) of 90° and a total twist angle (between each end) of 180°.

Figure 17 displays the moment-rotation relationship about the y axis for a three dimensional equal sense bend. From these initial tests the average equal sense peak moment (M_{-}^{max}) is 63Nmm and the average steady state moment (M_{-}^{*}) is 28Nmm.

Figure 18 displays the moment-rotation relationship about the x' axis for a three dimensional equal sense bend. From these experimental tests, it can be seen that the twist moment rises up to a peak value of 12.3Nmm. It can also be seen from figure 18 that the loading curve rises at both 10° and 40°, whereas the unloading curve is a smooth change in moment back to 0° rotation. This is due to the tape buckling at different twist angles when the rotational displacement was applied.

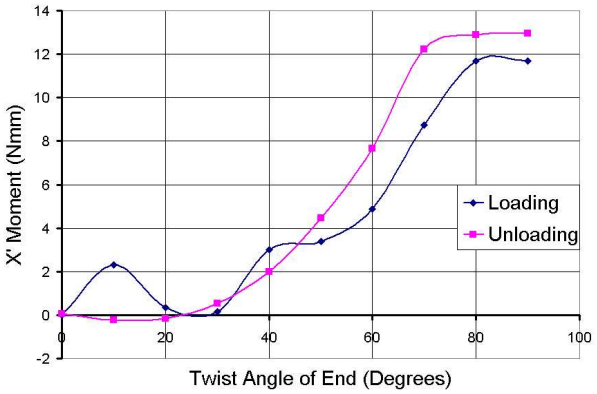

Fig. 18 Equal Sense 3D Twist Moment (End Twist Angle = 2 × End Bend Angle)

Theoretical Models

The accuracy of the experimental results was determined through a comparison with analytical analysis methods and finite element models.

Mathematical models simulating the bending of tape springs have previously been developed using shell theory. The development of such theory's can be found in Mansfield[4] (1973) and Seffen and Pellegrino[6] (1999). Approximate values for M_{+}^{*} and M_{-}^{*} for two dimensional bending can be found using equations 1 and 2.[6]

$$M_{+}^{*} = (1+\nu)D\alpha \tag{1}$$

$$M_{-}^{*} = -(1-\nu)D\alpha \tag{2}$$

Where, for the tape spring under test: $\nu = 0.3$, $D = 24.99Nmm^4$, $\alpha = 1.25$ rad.

Therefore, these equations predict M_{+}^{*} and M_{-}^{*} to be 40.6Nmm and -21.86Nmm respectively.

Mansfield[4] (1973) derives equations for both the longitudinal moment and twisting moment of the tape spring in terms of the longitudinal curvature (κ_x) and the twisting curvature (κ_{xy}). These curvatures are equivalent to the rotation angles. From this theoretical model it was found that M_{+}^{max} and M_{+}^{*} was calculated to be 248.4Nmm and 35.47Nmm respectively. This theory also predicts that the minimum torsional buckling moment of an equal sense fold is -20.46Nmm.

Various finite element models were also constructed in ANSYS to model both two dimensional and three dimensional tape spring folds.[7] The initial model, shown in figure 19, was constructed to analyze simple two dimensional bends. This figure shows the analysis of an opposite sense bend by applying a displacement at the center of the width (i.e. where y = 0) in the z direction. This model predicts the peak moment of an opposite sense fold (M_{+}^{max}) to be 340Nmm. The corresponding equal sense bend result (where the displacement is applied at the same node in the negative z direction) predicts that the peak equal sense moment (M_{-}^{max}) is -169Nmm. This, however, is the predicted equal sense buckling load of the tape spring failure due

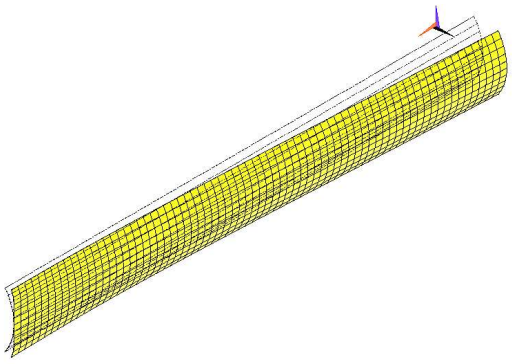

Fig. 19 Finite Element Model 1

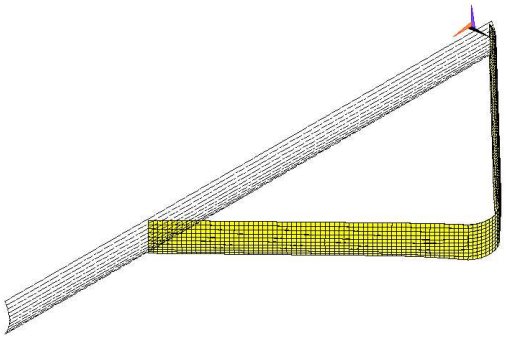

Fig. 20 Finite Element Model 2

to bending, not torsion. When displacements are applied on nodes where y > 0, (initiating a failure in the torsional mode) the buckling load reduces. A model was created with forty nodes across the width and the displacement was applied to the first node adjacent to the y = 0 centerline. The torsional buckling load was found to be -67.2Nmm.

The second model was constructed to more accurately simulate the motion of the tape spring during the experimental tests. This model can be seen in figure 20, folded into an equal sense bend. Two displacements were applied to this model at the edges of the width at half its length to form the fold shown in figure 20. The resultant central reaction force against central displacement plot can be seen in figure 21. This corresponds to a equal sense bend peak moment (M_{-}^{max}) of -108Nmm. However, this result is the minimum reaction load to bend the tape spring. Therefore, in this model, the tape spring does not fail in a torsional mode. This model also predicts the steady state moment of the fold (M_{-}^{*}) to be -22.68Nmm. The equivalent opposite sense model predicts a peak moment (M_{+}^{max}) of 343.5Nmm.

A simple finite element torsional model was set up to determine the approximate torsional loads expected from a tape spring twisted by 90°. The 20cm model is half the length of the tape spring tested experimentally. This model can be seen in figure 22. The corresponding reaction moment-rotational displacement graph is shown in figure 23. This model predicts a reaction moment of 8.41Nmm when the end is twisted by 90°.

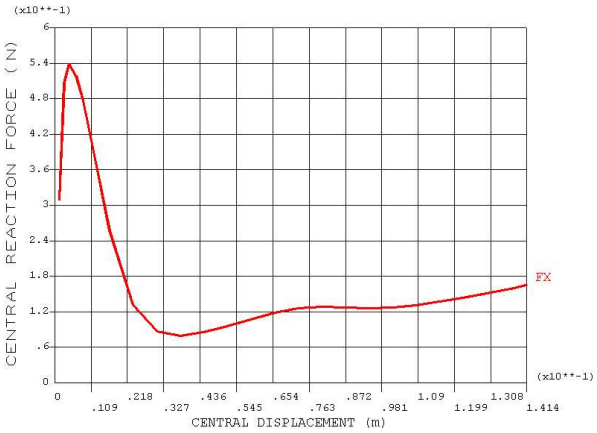

Fig. 21 Model 2 Equal Sense Result

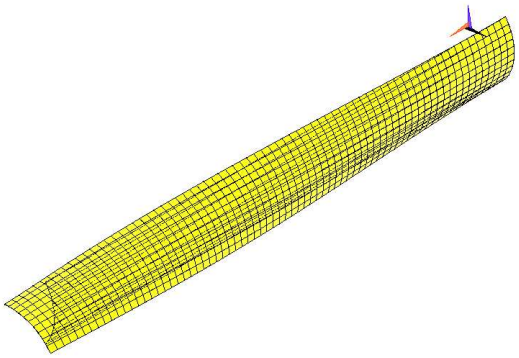

Fig. 22 Model 3 Basic Twist Simulation

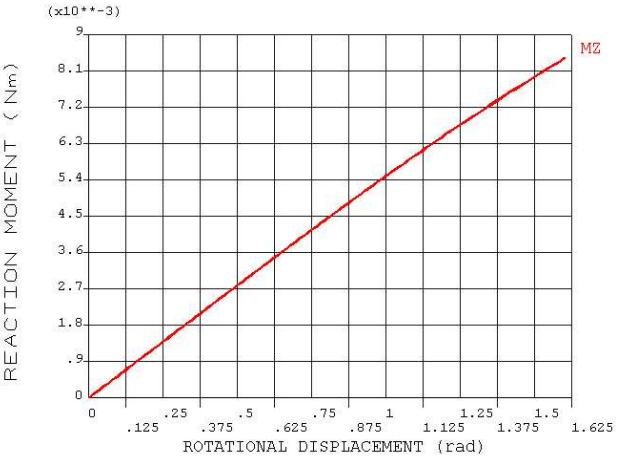

Fig. 23 Model 3 Twist Result

Results Comparison

A summary of the results is shown in tables 1, 2 and 3. From the 2D opposite sense bend results in table 1 it can be seen that the experimental result predicting M_{+}^{*} is very close to the theoretical values. As the experimental rig could not be used to determine M_{+}^{max}, no direct comparison can be made for this property. However, from Seffen (2000) it is found that the shell theory result tends to underestimate this parameter. This ref-

Result Method	M_{+}^{max} (Nmm)	M_{+}^{*} (Nmm)
Experimental	-	41.75
Basic Theory	-	40.60
Complex Theory	248.4	35.47
FEA Model 1	340.0	-
FEA Model 2	343.5	-

Table 1 2D Opposite Sense Bend Results Summary

Result Method	M_{-}^{max} (Nmm)	M_{-}^{*} (Nmm)
Experimental	-80.0	-23.25
Basic Theory	-	-21.86
Complex Theory	-20.46	-
FEA Model 1	-67.2	-
FEA Model 2	-108.0	-22.68

Table 2 2D Equal Sense Bend Results Summary

M_{-}^{max}	-63.0Nmm
M_{-}^{*}	-28.0Nmm
T^{max}	12.3Nmm

Table 3 Three Dimensional Experimental Results Summary

erence also shows that the finite element result tends to be close to the physical result. The results displayed here tend to agree with this concept as both finite element models predict almost identical values for M_{+}^{max} suggesting a true value of around 340Nmm. From the 2D equal sense bend results in table 2 it can be seen again that the experimental results for the steady state moment are very close to the theoretically predicted values. It is also shown that the complex shell theory result tends to match M_{-}^{*} closer than M_{-}^{max}. This is an expected result, as the same phenomenon can be found in Seffen[3] (2000). The results for M_{-}^{max} also show that the experimental result lies inbetween both finite element results. This is due to the fact that FEA model 2 is the minimum moment for a bending failure to occur, whereas FEA model 1 is the moment for a torsional failure to occur. However, this moment for torsional failure increases as the displacement loading becomes more symmetrical (tending towards a bending failure). The real value for M_{-}^{max} would be within the range of -67.2 to -108.0Nmm. Therefore the experimental result is found to be quite accurate as it lies close to the center of this predicted range.

The three dimensional bending results (seen in table 3) show that the peak moment occurs at a lower magnitude than the two dimensional result. This is the expected result as the applied twist reduces the buckling load for buckling in the torsional mode. It can also be seen from the results that the presence of the twist in the tape spring has increased the steady state moment of the bend.

Experimental results have shown that the twisting moment rises as shown in figure 18 to 12.3Nmm. The simple finite element model for a straight tape predicts

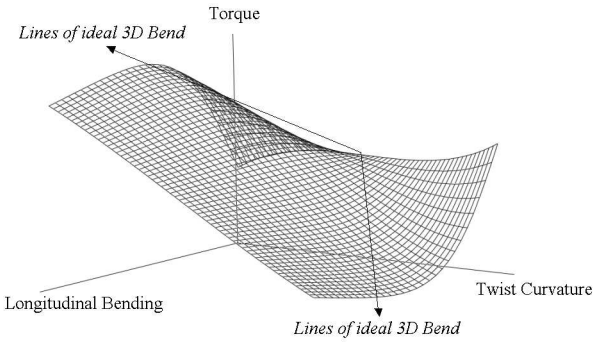

Fig. 24 Shell Theory Torque Model

that the twisting moment rises as shown in figure 23 to 8.41Nmm. A comparison between these two graphs suggests that the experimental twist moment at small twist angles of a longitudinally bent tape spring is less than the twist moment for a straight tape. Conversely, the experimental twist moment at large twist angles of a longitudinally bent tape spring is greater than the twist moment for a straight tape. This result is confirmed by the theoretical torsion relationship shown in Mansfield[4] (1973). A plot of this relationship is shown in figure 24. This figure shows how the predicted torque changes with increasing longitudinal bending. The three dimensional experimental testing that has been performed was on ideal 3D bends (i.e. incrementing the test strip uniformly with 5° of bending and 10° of twist). It can be seen that the theory, along these lines of ideal 3D bends follows the same path as produced by the experimental results.

Conclusions

This work has focused on using tape springs to support a new conceptual area deployment design for nano/micro satellites. The deployment of this design incorporates bi-axial folding, which requires the tape springs to unfold in three dimensions. The design of a test rig to determine the properties of this three dimensional deployment has been presented. This rig measures both the bending and twisting moments produced from the three-dimensional fold. The combination of these two moments defines the main deployment properties of the tape spring and hence the final array. The results produced from early experimental tests have been presented along with a comparison with the theoretical models. The theoretical models consisted of existing relationships derived from shell theory and finite element analysis models using ANSYS. During these initial tests, some unexpected discrepancies were found in the system and work is currently being performed to overcome them. However, despite these issues, the test results show that the system is very capable of producing accurate moment results for both two and three dimensional tape spring bends.

References

[1]C.C. Liebe, S. M., "MEMS based sun sensor," *IEEE Aerospace Conference Proceedings*, Vol. 3, 2001, pp. 31565–31572.

[2]S.J.I. Walker, G. A., "An application of Tape Springs in Small Satellite Area Deployment Devices," *Proceedings of 5th International Conference on Dynamics and Control of Systems and Structures in Space*, 2002.

[3]K. A. Seffen, Z. You, S. P., "Folding and deployment of curved tape springs," *International Journal of Mechanical Sciences*, Vol. 42, 2000, pp. 2055–2073.

[4]Mansfield, E. H., "Large-deflection torsion and flexure of initially curved strips," *Proc. Roy. Soc. Lond.*, Vol. A. 334, 1973, pp. 279–298.

[5]Fischer, A., "Bending instabilities of thin-walled transversly curved metallic springs," *Cambridge University Engineering Department*, Vol. CUED/D-STRUCT/TR 154, 1995.

[6]K. A. Seffen, S. P., "Deployment dynamics of tape springs," *Proc. Roy. Soc. Lond.*, Vol. A 455, 1999, pp. 1003–1048.

[7]Moaveni, S., *Finite Element Analysis: Theory and Application with ANSYS*, Prentice Hall, 1999, ISBN: 0137850980.